

## CONFORMATIONAL SPACE AND ELECTRONIC ABSORPTION PROPERTIES OF THE TWO ISOMERS OF RESVERATROL

RÉKA-ANITA DOMOKOS<sup>1</sup>, V. CHIŞ<sup>1\*</sup>

**ABSTRACT.** The present study analyses the *trans* and *cis* conformations of resveratrol, aiming to get clear experimental and computational evidences that can be used to differentiate between the two isomers. Three conformers for each isomer have been considered and their characteristic geometrical parameters, relative free energies, Boltzmann populations and electronic transitions have been calculated at B3LYP/6-31+G(2d,2p) level of theory in gas phase, as well as in water, ethanol and DMSO. The experimental UV-Vis spectra of the two isomers have been explained by using the time dependent density functional theory (TD-DFT) formalism.

**Keywords:** *trans-resveratrol; cis-resveratrol; conformational analysis; UV-VIS*

---

<sup>1</sup> Babeş-Bolyai University, Faculty of Physics, 1 Kogălniceanu, RO-400084 Cluj-Napoca, Romania

\* Corresponding author: [vasile.chis@phys.ubbcluj.ro](mailto:vasile.chis@phys.ubbcluj.ro)

## INTRODUCTION

Resveratrol (3, 5, 4'- trihydroxystilbene - RESV) has been proven to be a strong antioxidant and anti-inflammatory compound, showing also beneficial effects for treating diseases like heart failure, breast and prostate cancers, stroke, brain damage, etc. [1-4]. RESV is found in red grapes and wine [5] and it is widely believed to be responsible for the "French Paradox" which describe the low incidence of heart disease and obesity among the French in contrast to their relatively high-fat diet [6]. The structure of RESV consists of two phenols linked by a double bond which facilitates two isomeric forms, called *trans*- (E) - and *cis*- (Z) resveratrol (Fig. 1). The biological activity of RESV seems to be primarily due to its *trans*-isomer, while the *cis* isomer is obtained by UV-irradiation of the *trans*-RESV [7].

In spite of its structural simplicity and of a wealth of spectroscopically data reported in the literature about RESV, its structural isomers, particularly the *cis* form, have not been yet fully characterized.

The solid state structure of *trans*-resveratrol was studied by X-Ray technique [8] being shown that these molecules in solid phase are interconnected by an extensive hydrogen bond network. On the other hand, to the best of our knowledge, no information related to structural parameters of the *cis* isomer has been reported so far.

The spectroscopic response of various isomers of a compound can be significantly different. This is particularly important for UV-VIS spectra, but also for other spectroscopic techniques. That's why we analyzed in this study the two isomeric forms of resveratrol, aiming to get clear experimental and computational evidences that can be used to differentiate between the two conformers. In order to obtain new information about the structure and the electronic properties of both isomers, this study has been conducted using the UV-VIS spectroscopy coupled to methods of computational spectroscopy based on DFT and TD-DFT formalisms. Molecular structures of the isomers and their energetic stability was investigated in gas phase, as well as in liquid phase (ethanol, water and DMSO).

## EXPERIMENTAL AND COMPUTATIONAL DETAILS

The two isomeric forms (*trans* (E-) and *cis* (Z-)) of RESV compound were purchased from Cayman Chemical and used as received. *Trans*-resveratrol was supplied in powder form with a purity  $\geq 98\%$  and *cis*-resveratrol as a solution in ethanol with a purity  $\geq 98\%$ .

Optical absorbance spectra of the two isomers were recorded at room temperature using a Jasco V-630 UV-Vis double beam spectrophotometer with a slit width of 2 nm. The spectra of both isomers have been recorded in ethanol at different concentration.

Geometry optimizations and single point calculations were performed with the Gaussian 09, revision E.01 software package [9] by using DFT approaches. The hybrid B3LYP exchange-correlation functional [10-12] was used in conjunction with Pople's split valence 6-31+G(2d,2p) basis set [13-14]. Absorption spectra for both isomer of RESV were calculated using the time-dependent DFT (TD-DFT) methodology [15], implemented in the Gaussian09 package. The simulated UV-vis spectrum of RESV in the 180–500 nm range has been obtained by summation of the contributions from transitions to the first 30 singlet excited electronic states. The UV spectral line-shapes were convoluted with Gaussian functions with the full width at half maximum of 0.33 eV. The nature of the excited states has been analyzed using the Natural Transition Orbitals (NTO) formalism [16].

Solvent effects on the vertical excitation energies were also considered by using the implicit Polarizable Continuum Model (PCM) of solvation [17].

## RESULTS AND DISCUSSIONS

Our first interest was to investigate the stability of the possible conformers of RESV in both isomeric forms. The starting geometries of *trans*-RESV used for geometry optimizations were derived from the X-ray

diffraction data reported by Caruso *et al.* [8]. For *cis*-RESV the starting geometries were obtained by a dihedral distortion of the *trans* isomer around the C7-C8 olefin bond (see atom numbering scheme in Fig. 1).

Depending on the mutual orientation of the OH bonds in RESV, three different conformers have been analyzed for each isomer and they are shown in Fig. 1. A good agreement is observed between the solid state structure of *trans*-RESV and that of its *c2* conformer in gas-phase. Thus, the shortest calculated bond for the *c2-trans*-RESV (1.348 Å) is the olefin C7=C8 bond, as it was also observed in solid state, where the corresponding bond length is 1.333 Å [8]. It remains the shortest bond for all conformers of the two isomers, with values in the 1.349-1.350 Å interval. The calculated aromatic CC bond lengths are between 1.387 – 1.409 Å (1.37 – 1.40 Å – experimental) and the calculated longest bonds correspond to the olefin-phenyl bonds, 1.466 Å for the C1-C7 bond and 1.463 Å for the C8-C9 bond (experimental values are 1.468 Å and 1.460 Å, respectively [8]). All the C-O bonds are predicted longer by calculations and this fact can be explained by the extended network of hydrogen bonds in which the OH groups are involved in solid state.

The calculations reproduce also very well the non-planarity of this isomer. Thus, the calculated dihedrals that give the non-coplanarity of the olefin moiety with the two phenyl rings are 5.97° and 4.97° for di-*m*-OH and *p*-OH rings, respectively. The calculated dihedral angle between the planes defined by the two rings is 11.06 Å, slightly larger than the experimental value (5.30 Å [8]). Solid state structure of *trans*-RESV shows that the two hydroxyl groups in the di-*m*-OH phenyl are almost coplanar with the ring, while in case of *p*-OH phenyl ring the OH bond is out of plane by 51.09° [8]. However, since the intermolecular hydrogen bond interactions were not considered in this study, for the isolated *trans*-RESV molecule, the three OH bonds are predicted coplanar with the phenyl rings, for all the conformers of *trans*-RESV, both in gas-phase and in solution.

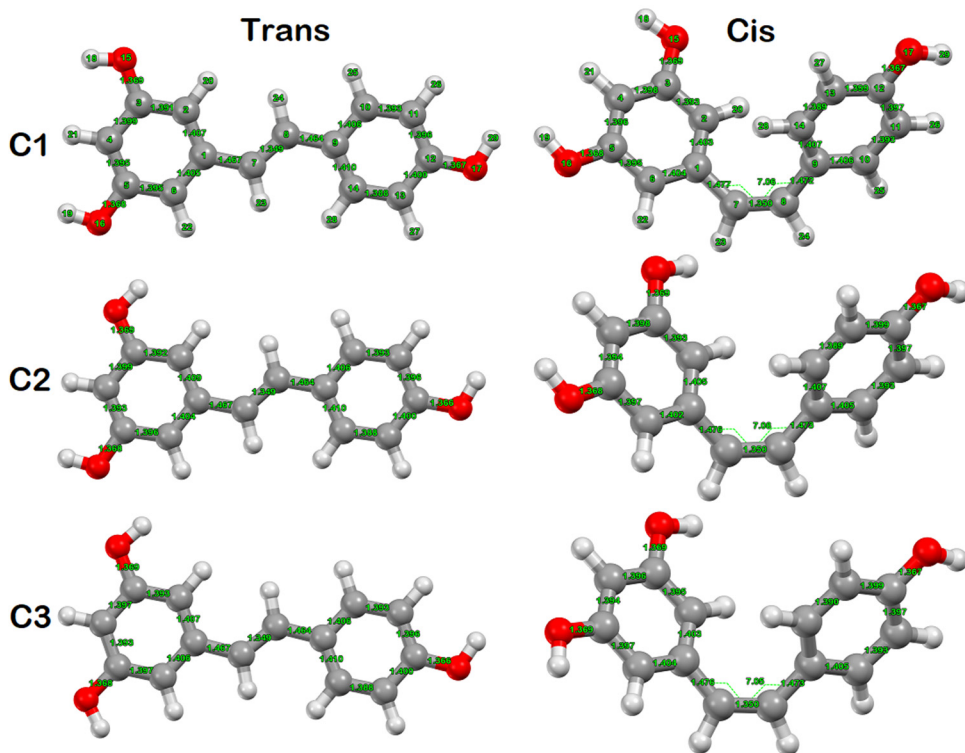


**Fig. 1.** PCM-B3LYP/6-31+G(2d,2p) optimized geometries of *trans*- (left) and *cis*- (right) resveratrol in ethanol

The calculated geometrical parameters for all the three conformers of the *trans*- and *cis*-RESV in ethanol are shown in Fig. 1. Computational data show that for the conformers of both isomers, the bond lengths as well as the valence and dihedral angles suffer minor changes between the gas and solution phases.

Comparing the geometrical parameters of the two isomers, as expected, the most pronounced differences were observed for the C1-C7 and C9-C10 bonds which become slightly longer for the *cis* isomer. It is worth noting that the C7=C8 double bond remains practically unchanged between the isomers and does not change also as a result of transition between the gas and liquid states.

Moreover, the most important changes of the valence angles (however, less than  $5^\circ$ ) are predicted by calculations for the C2-C3-O15 and C1-C7-C5 angles. The first one decreases by  $5^\circ$ , while the latter increases by about  $4^\circ$  when going from the *trans*- to the *cis* isomer.

Obviously, the largest changes between the isomers are observed for the dihedral angles defining the orientation of the two phenyl rings relative to olefin moiety. Thus, the C1-C7-C8-C9 dihedral angle changes from  $180^\circ$  for the *trans* isomer to  $7^\circ$  in case of *cis* conformation. In ethanol, the deviation from the Ph-olefin coplanarity, characteristic for the *trans* isomer, is predicted to be of  $37.8^\circ$  for the di-*m*-OH phenyl and  $27.1^\circ$  for the *p*-OH phenyl, in case of the *cis* isomer. Similar distortions were predicted in gas phase.

### 2D and 1D potential energy surfaces (PESs) of Resveratrol

The relaxed 2D PES of resveratrol in gas-phase (Fig. 2) has been calculated at B3LYP/STO-3G level of theory, by varying the C6-C1-C7-C8 and C7-C8-C9-C10 dihedrals (marked with a star in the left upper corner of Fig.2) in steps of  $10^\circ$ , within the  $0 \div 180^\circ$  interval.

Two stationary points have been identified on the 2D PES; the global minimum ( $GM_{2D}$ ) is four-fold degenerate due to the symmetry of the molecule and it corresponds to the *trans* isomer. The same is true for the saddle point ( $SP_{2D}$ ) which adopts a structure with the two phenyl rings making a dihedral angle of  $80.1^\circ$ . The global maximum ( $MAX_{2D}$ ) has a stair-like structure, with the planes of the phenyl rings being parallel and the plane containing the olefin bond perpendicular to the phenyl rings.

The energetic difference between the  $GM_{2D}$  and  $SP_{2D}$  is 5.65 kcal/mol, and the  $MAX_{2D}$  structure is 6.28 kcal/mol above the  $SP_{2D}$ .

However, none of the points of the 2D PES corresponds to the *cis* isomeric form. Such a structure can only be obtained by performing a rotational scan around the C=C bond. The relaxed 1D PES in ethanol has been obtained by varying the H23-C7-C8-H24 dihedral with a step of  $10^\circ$ , within the  $-180^\circ \div 180^\circ$  interval (see Fig. 3).

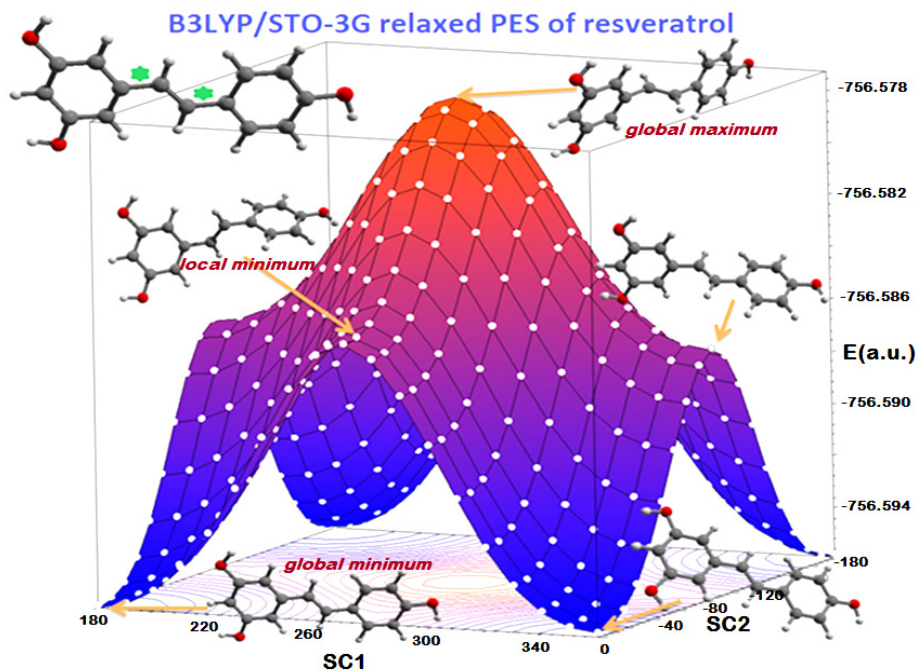


**Fig. 2.** Relaxed 2D PES of *trans*-RESV (c2 conformer) calculated at B3LYP/STO-3G level of theory, in gas-phase

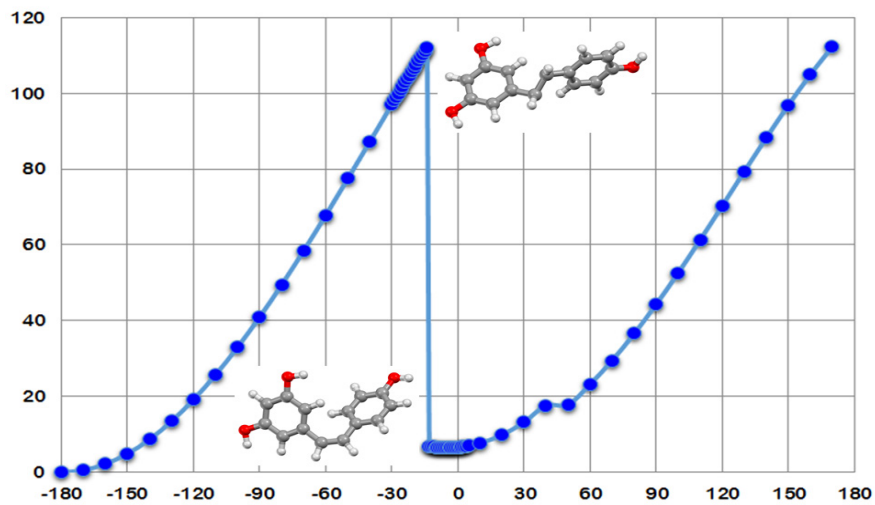


**Fig. 3.** Relaxed 1D PES of *trans*-RESV (c3 conformer) calculated at PCM-B3LYP/STO-3G level of theory, in ethanol

The step was reduced to  $1^\circ$  for the  $-30^\circ \div 0^\circ$  interval, where the transition from *trans* to *cis* occurs. We used the c3 conformer of the RESV because it is the lowest energy conformer in liquid phase for both isomers (see Table 1). Again, two stationary points have been obtained on the 1D PES, the global minimum ( $GM_{1D}$ ) corresponding to the *trans*-RESV and another, local minimum ( $LM_{1D}$ ), for the value of  $-5^\circ$  of the H23-C7-C8-H24 scanning dihedral angle, which corresponds to the *cis* isomer. The maximum energy structure on the 1D PES in ethanol ( $MAX_{1D}$ ) is 106.67 kcal/mol higher in energy than the *trans* isomer and 99.77 kcal/mol than the *cis*-RESV. The angles between the phenyl rings of the *cis* isomer and  $MAX_{1D}$  structures are  $48.64^\circ$  and  $84.07^\circ$ , respectively. Even though the *cis* and *trans* isomers are separated only by 6.9 kcal/mol, the energetic barrier between the two isomers is 106.67 kcal/mol which corresponds to a wavelength of 268 nm. This value is in excellent agreement with the results of Figueiras et al. [7] who used a wavelength of 260 nm for inducing the *trans-cis* photo-isomerization of resveratrol.

As shown in Table 1, our calculations predict a small change of the relative energies of the conformers when going from gas phase to liquid phase. The three studied conformer of both isomers are very close in energy in gas phase, as well as in liquid phase (ethanol, water and DMSO). The conformer c2 of both isomeric forms are the most stable in gas phase, but, contrary to the *trans* isomer, in case of the *cis* isomer, the c3 conformer is very close in energy to c2. On the other hand, in solutions, the c3 conformers are most stable, but c2 conformers also have comparable Boltzmann populations, particularly for the *trans* isomer.

The calculated UV-Vis spectra for the three conformers of *trans* (or *cis*) isomer (not shown) are very similar. Thus, for instance, in case of *trans*-RESV in ethanol, the calculated  $\lambda_{max}$  varies between 342.89 nm for c1 and 343.97 nm for c3, that is, in the limit of experimental errors. For the *cis* conformers,  $\lambda_{max}$  was calculated between 327.55 nm for c2 and 328.25 nm for c3.



**Table 1.** Relative Gibbs energies ( $\Delta G$ , kcal mol<sup>-1</sup>) and Boltzmann populations (%) of the three conformers of *trans*- and *cis*-RESV optimized in gas phase, ethanol, water and DMSO solutions, at room temperature

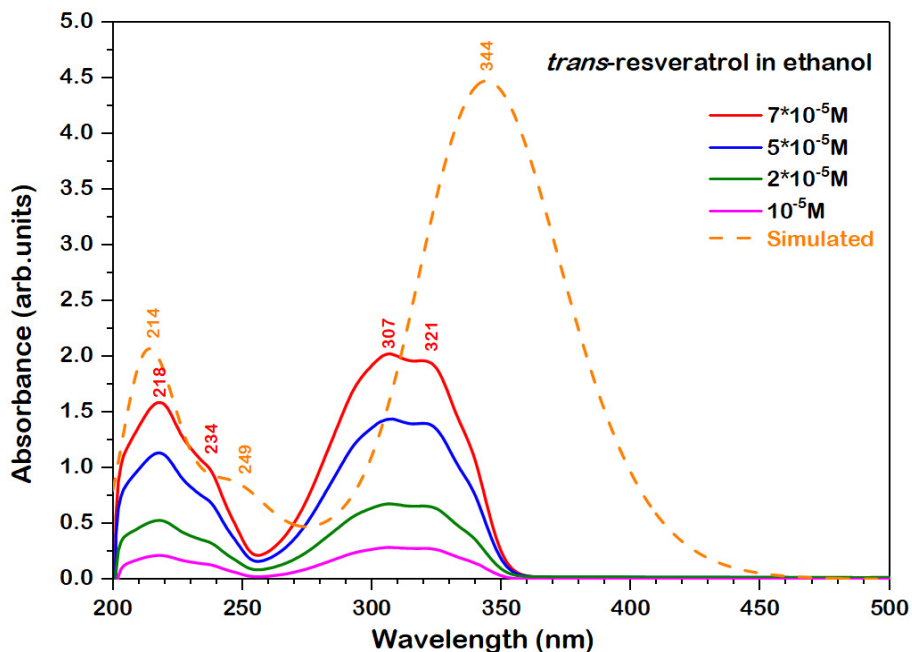
	gas-phase		ethanol		water		DMSO	
	$\Delta G$	Population	$\Delta G$	Population	$\Delta G$	Population	$\Delta G$	Population
<b><i>trans</i>-RESV</b>								
c1	0.648	17.95%	0.239	25.42%	0.285	24.27%	0.270	24.61%
c2	0.000	53.59%	0.024	36.52%	0.043	36.48%	0.036	36.54%
c3	0.375	28.46%	0.000	38.06%	0.000	39.25%	0.000	38.85%
<b><i>cis</i>-RESV</b>								
c1	0.894	10.26%	0.380	21.94%	0.352	22.88%	0.362	22.56%
c2	0.000	46.38%	0.080	36.40%	0.089	35.67%	0.087	35.88%
c3	0.040	43.36%	0.000	41.66%	0.000	41.45%	0.000	41.57%

For this reason we calculated the electronic absorption of both isomeric forms of resveratrol molecules considering the most stable conformation and those with the highest relative populations in ethanol.

The UV-Vis spectra of *trans*-resveratrol in ethanol (Fig. 4) were recorded at four concentrations, ranging from  $7 \cdot 10^{-5}$  M to  $10^{-5}$  M. As can be seen in Figure 4, the UV-Vis spectrum of *trans*-resveratrol consists of four peaks (218, 234, 307 and 321 nm) and their position does not change by varying the concentration.

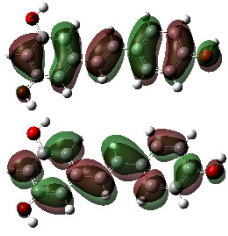
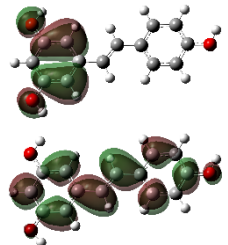
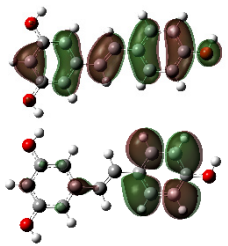
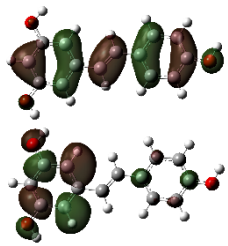
The calculated transition energy values and the transition types of *trans*-resveratrol are summarized in Table 2. The first excited state of the *trans*-resveratrol isomer results from the HOMO  $\rightarrow$  LUMO transition (99%). The calculated value for the electron transition with the smallest energy corresponds to  $\lambda_{\max}=344$  nm, which is higher than the experimentally determined value by cca. 30 nm. Such differences are frequently reported in the literature [18] and they are due to the approximations used in these calculations. On the other hand, the peak at 218 nm is in excellent agreement

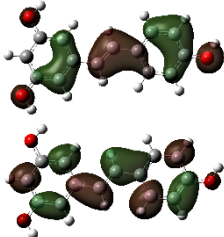
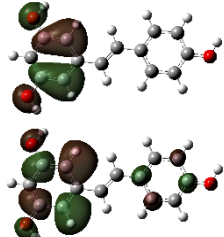
with the experimental value and corresponds to a HOMO-4  $\rightarrow$  LUMO transition. The other experimentally determined peaks are displaced from those theoretically predicted by less than 15 nm. Thus, the experimental bands at 321, 307 and 234 nm correspond to the calculated value of 314 nm, 287 and 232 nm, respectively. The theoretical absorption spectrum of the *trans*-resveratrol molecule (Figure 4, dashed line) reproduces satisfactory all the features of the experimental spectra, both the bands positions and their relative intensities.



**Fig. 4.** Experimental UV-VIS spectrum of the *trans*-resveratrol in ethanol at different concentration and the simulated UV-VIS spectrum of its c3 conformer in ethanol at PCM-TD-B3LYP/6-31+G(2d,2p) level of theory

**Table 2.** PCM-B3LYP/6-31+G(2d,2p) calculated electronic transitions for the c3 conformer of *trans*-resveratrol in ethanol

Excited state	$\lambda$ (nm)	f	Transitions	Contributions * (%)	NTOs** Coefficient/Shape
1	343.97	1.0709	H->L	98.99	0.999 
2	312.36	0.0391	H-1->L	92.90	0.933 
3	286.60	0.0782	H->L+1	82.62	0.840 
6	248.27	0.1278	H->L+3	71.01	0.751 

Excited state	$\lambda$ (nm)	f	Transitions	Contributions * (%)	NTOs** Coefficient/Shape
16	217.40	0.1342	H-4->L	42.45	0.480 
19	210.66	0.3182	H-1->L+3	75.90	0.784 

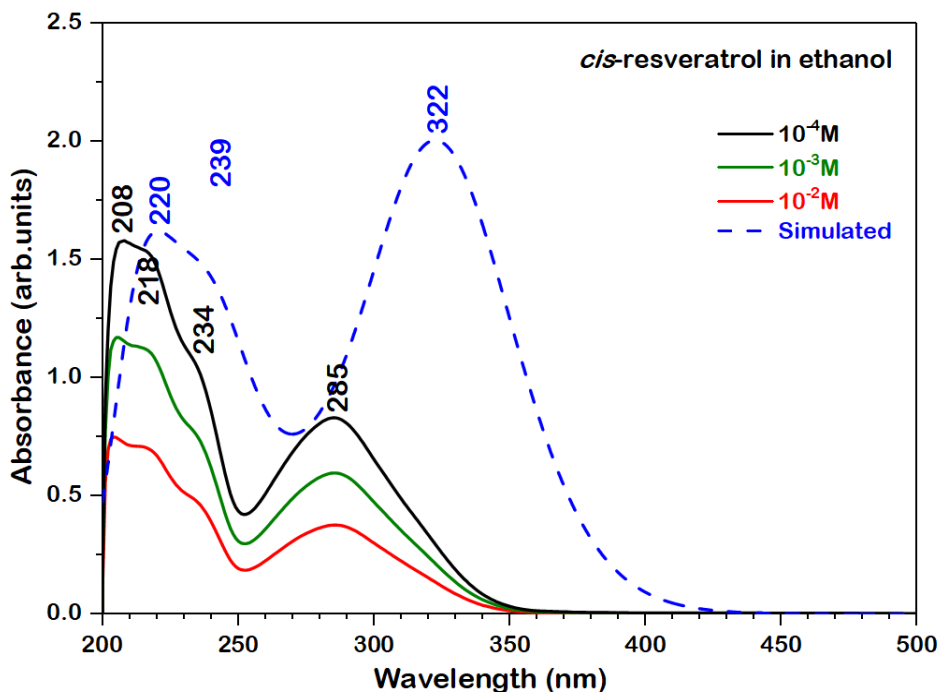
\*Only the largest contribution is included

\*\*HOTO - left and LUTO – right (isovalue 0.02 a.u.); The NTO coefficients represent the extent to which the excitation can be written as a single configuration [19].

As shown in the last column of Table 2, the first excited state appears as a result of a  $\pi \rightarrow \pi^*$  transition, while the transitions to the excited states 2, 3 and 6 correspond to intra-molecular charge transfers, in each case, the HOTOs and LUTOs being localized on different parts of the molecule. The last two calculated transitions are mainly due to a redistribution of electronic charge within the molecule.

Analogously was studied the *cis*-resveratrol isomer, its absorption spectrum being shown in Figure 5. Four absorption bands can be identified in the experimental spectrum at 204-208 nm, 211 nm, 232 nm and 285-286 nm. Compared to the *trans* isomer, the experimental  $\lambda_{\max}$  for *cis*-RESV is blue-

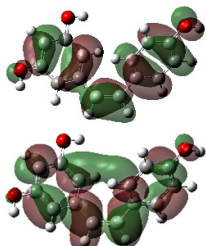
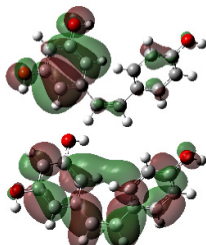
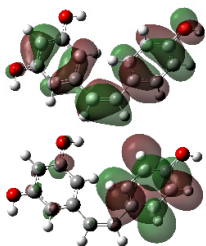
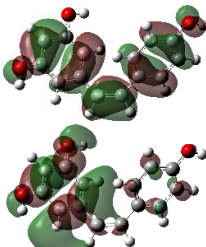
shifted by 30 nm and less intense than the bands observed in the 204-232 nm. The two isomers show distinct UV-Vis spectra, differing both in the positions of the bands, but also in their relative intensities.

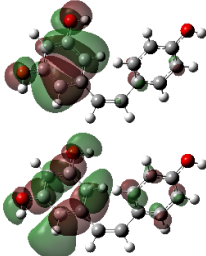
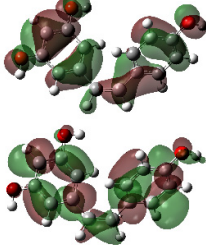


**Fig. 5.** Experimental UV-VIS spectrum of the *cis*-resveratrol in ethanol at different concentration and the simulated UV-Vis spectrum of its c3 conformer in ethanol at PCM-TD-B3LYP/6-31+G(2d,2p) level of theory

The assignments of the electronic transitions of *cis*-RESV are given in Table 3. The lowest excited state for *cis*-RESV appears as a result of HOMO → LUMO transition (97.08% contribution), similar to the case of *trans* isomer. Again, a discrepancy of 37 nm was noted between the experimental and calculated  $\lambda_{\max}$  band.

**Table 3.** PCM-B3LYP/6-31+G(2d,2p) calculated electronic transitions for the c3 conformer of *cis*-resveratrol in ethanol

Excited state	$\lambda$ (nm)	f	Transitions	Contributions* (%)	NTOs** Coefficient/Shape
1	328.25	0.4145	H->L	97.08	0.996 
2	302.25	0.0914	H-1->L	89.48	0.913 
3	279.34	0.1054	H->L+1	80.12	0.819 
6	245.20	0.1196	H->L+4	28.28	0.503 

Excited state	$\lambda$ (nm)	f	Transitions	Contributions* (%)	NTOs** Coefficient/Shape
19	210.96	0.1230	H-1->L+4	39.28	0.489 
25	201.17	0.1910	H-2->L+3	47.16	0.719 

\*Only the largest contribution is included

\*\*HOTO - left and LUTO – right (isovalue 0.02 a.u.). The NTO coefficients represent the extent to which the excitation can be written as a single configuration [19].

The first absorption band experimentally determined at 204-208 nm was not reproduced by calculations. On the other hand, a very good agreement was obtained between the experimental and theoretical excitation energies (especially at 216 nm and 234 nm), the differences being within the limit of the experimental errors. The 216 nm and 234 nm experimental absorption bands are in excellent agreement with those determined theoretically (211 nm and 245 nm, respectively). The first corresponds to the HOMO-1  $\rightarrow$  LUMO+4 transition and the second results from the HOMO  $\rightarrow$  LUMO+4 transition.

Like in the case of *trans* isomer, the lowest excited state of *cis*-RESV is due to the HOMO-LUMO transition of  $\pi$ - $\pi^*$  type. However, as seen in Tables 2 and 3, while the LUMO of the *trans*-RESV is bonding with respect to the C=C double bond, it becomes anti-bonding for the *cis* isomer. This character leads to an increase of its energy for *cis* and, consequently to a higher energy HOMO-LUMO gap and lower  $\lambda_{\max}$ .

The next three transitions with appreciable oscillator strength are due to an intra-molecular charge transfer in the molecule. Also, the last two calculated transitions are again due to a redistribution of electronic charge within the molecule.

## CONCLUSIONS

Here we analyzed the stability of the two isomers of resveratrol, as well as the relative energies of their possible conformers, determined by the relative orientation of the OH groups, in gas-phase as well as in ethanol, water and DMSO solutions at the B3LYP/6-31+G(2d,2p) level of theory.

Three conformers have been identified for each isomer, within a 0 ÷ 0.65 kcal/mol and 0 ÷ 0.29 kcal/mol energy window, in gas-phase and liquid phase, respectively for the *trans* isomer, while for the *cis* partner the corresponding Gibbs free energy intervals were 0 ÷ 0.89 kcal/mol in gas-phase and 0 ÷ 0.38 kcal/mol in solutions. The geometrical parameters of the conformers of each isomer are slightly affected when passing from the gas- to liquid phases.

Conformer 2 is the most stable for both isomeric forms in gas-phase, while the conformer c3 become the most stabilized in water, ethanol and DMSO. However, either in gas-phase or in solutions, the other two conformers are also appreciably populated at room temperature. On the other hand, the conformers of the *cis* isomer are more than 6 kcal·mol<sup>-1</sup> higher in energy than those of the *trans*- partner.



Two stationary points have been obtained on the 1D PES of RESV in ethanol, corresponding to the *trans* and *cis* isomers, separated by 6.9 kcal/mol. Nevertheless, the energetic barrier between the two isomers is 106.67 kcal/mol, a value which corresponds to a wavelength of 268 nm.

The two isomers show distinct UV-Vis spectra differing in the positions of the  $\lambda_{\max}$ , which is red-shifted for *trans* by 30 nm, but also in its relative intensity with respect to the other absorption peaks. Experimental absorption spectra have been accurately reproduced by TD-DFT calculations and using the NTO it was proved that the lowest excited states are due to  $\pi$ - $\pi^*$  transitions. However, the LUMO orbital changed from bonding to antibonding with respect to the C=C double bond when passing from *trans* to *cis* isomer, causing a lower  $\lambda_{\max}$  for the *cis* isomer.

## ACKNOWLEDGEMENTS

The research undertaken for this article was conducted using the Babeş-Bolyai University Research infrastructure financed by the Romanian Government through the project MADECIP (POSCEE COD SMIS CSNR 48801/1862).

R.A. DOMOKOS highly acknowledges financial support from the Babeş-Bolyai University through a Performance Scholarship during the academic year 2015–2016, contract number 35218/11.11.2015.

## REFERENCES

1. J. Gusman, H. Malonne, and G. Atassi, "A reappraisal of the potential chemopreventive and chemotherapeutic properties of resveratrol," *Carcinogenesis*, 22 (2001) 1111–1117.
2. S. Quideau, D. Deffieux, and L. Pouységu, "Resveratrol Still Has Something To Say about Aging!," *Angew. Chem. Int. Ed.*, vol. 51, no. 28, pp. 6824–6826, Jul. 2012.

3. R.Á. Rodríguez, I.R. Lahoz, O.N. Faza, M.M. Cid, and C.S. Lopez, "Theoretical and experimental exploration of the photochemistry of resveratrol: beyond the simple double bond isomerization," *Org. Biomol. Chem.*, vol. 10, no. 46, pp. 9175–9182, Nov. 2012.
4. M. Diaz, H. Degens, L. Vanhees, C. Austin, and M. Azzawi, "The effects of resveratrol on aging vessels," *Exp. Gerontol.*, vol. 85, no. Supplement C, pp. 41–47, Dec. 2016.
5. J. Park and Y.C. Boo, "Isolation of Resveratrol from *Vitis Viniferae* Caulis and Its Potent Inhibition of Human Tyrosinase," *Evidence-Based Complementary and Alternative Medicine*, 2013. [Online]. Available: <https://www.hindawi.com/journals/ecam/2013/645257/>. [Accessed: 13-Dec-2017].
6. S. Renaud and M. de Lorgeril, "Wine, alcohol, platelets, and the French paradox for coronary heart disease," *Orig. Publ.*, Vol. 1, Issue 8808, vol. 339, no. 8808, pp. 1523–1526, Jun. 1992.
7. T.S. Figueiras, M.T. Neves-Petersen, and S.B. Petersen, "Activation energy of light induced isomerization of resveratrol," *J. Fluoresc.*, vol. 21, no. 5, pp. 1897–1906, Sep. 2011.
8. F. Caruso, J. Tanski, A. Villegas-Estrada, and M. Rossi, "Structural Basis for Antioxidant Activity of trans-Resveratrol: Ab Initio Calculations and Crystal and Molecular Structure," *J. Agric. Food Chem.*, vol. 52, no. 24, pp. 7279–7285, Dec. 2004.
9. Gaussian 09, Revision E.01, M.J. Frisch, G. W. Trucks, H. B. Schlegel, G. E. Scuseria, M. A. Robb, J. R. Cheeseman, G. Scalmani, V. Barone, G.A. Petersson, H. Nakatsuji, X. Li, M. Caricato, A. Marenich, J. Bloino, B.G. Janesko, R. Gomperts, B. Mennucci, H.P. Hratchian, J.V. Ortiz, A.F. Izmaylov, J.L. Sonnenberg, D. Williams-Young, F. Ding, F. Lipparini, F. Egidi, J. Goings, B. Peng, A. Petrone, T. Henderson, D. Ranasinghe, V.G. Zakrzewski, J. Gao, N. Rega, G. Zheng, W. Liang, M. Hada, M. Ehara, K. Toyota, R. Fukuda, J. Hasegawa, M. Ishida, T. Nakajima, Y. Honda, O. Kitao, H. Nakai, T. Vreven, K. Throssell, J.A. Montgomery, Jr., J.E. Peralta, F. Ogliaro, M. Bearpark, J.J. Heyd, E. Brothers, K.N. Kudin, V.N. Staroverov, T. Keith, R. Kobayashi, J. Normand, K. Raghavachari, A. Rendell, J.C. Burant, S.S. Iyengar, J. Tomasi, M. Cossi, J.M. Millam, M. Klene, C. Adamo, R. Cammi, J.W. Ochterski, R.L. Martin, K. Morokuma, O. Farkas, J.B. Foresman, and D. J. Fox, Gaussian, Inc., Wallingford CT, 2016.

10. A.D. Becke, "Density-functional thermochemistry. III. The role of exact exchange," *J. Chem. Phys.*, vol. 98, no. 7, pp. 5648–5652, Apr. 1993.
11. C. Lee, W. Yang, and R.G. Parr, "Development of the Colle-Salvetti correlation-energy formula into a functional of the electron density," *Phys. Rev. B*, vol. 37, no. 2, pp. 785–789, Jan. 1988.
12. S.H. Vosko, L. Wilk, and M. Nusair, "Accurate spin-dependent electron liquid correlation energies for local spin density calculations: a critical analysis," *Can. J. Phys.*, vol. 58, no. 8, pp. 1200–1211, Aug. 1980.
13. W.J. Hehre, R. Ditchfield, and J.A. Pople, "Self-Consistent Molecular Orbital Methods. XII. Further Extensions of Gaussian-Type Basis Sets for Use in Molecular Orbital Studies of Organic Molecules," *J. Chem. Phys.*, vol. 56, no. 5, pp. 2257–2261, Mar. 1972.
14. M.J. Frisch, J.A. Pople, and J. S. Binkley, "Self-consistent molecular orbital methods 25. Supplementary functions for Gaussian basis sets," *J. Chem. Phys.*, vol. 80, no. 7, pp. 3265–3269, Apr. 1984.
15. M.E. Casida, C. Jamorski, K.C. Casida, and D.R. Salahub, "Molecular excitation energies to high-lying bound states from time-dependent density-functional response theory: Characterization and correction of the time-dependent local density approximation ionization threshold," *J. Chem. Phys.*, vol. 108, no. 11, pp. 4439–4449, Mar. 1998.
16. R.L. Martin, "Natural transition orbitals," *J. Chem. Phys.*, vol. 118, no. 11, pp. 4775–4777, Feb. 2003.
17. J. Tomasi, B. Mennucci, and R. Cammi, "Quantum Mechanical Continuum Solvation Models," *Chem. Rev.*, vol. 105, no. 8, pp. 2999–3094, Aug. 2005.
18. A.J. Cohen, P. Mori-Sánchez, and W. Yang, "Challenges for Density Functional Theory," *Chem. Rev.*, vol. 112, no. 1, pp. 289–320, Jan. 2012.
19. A.E. Clark, "Time-Dependent Density Functional Theory Studies of the Photoswitching of the Two-Photon Absorption Spectra in Stilbene, Metacyclopentadiene, and Diarylethene Chromophores," *J. Phys. Chem. A*, vol. 110, no. 10, pp. 3790–3796, Mar. 2006.

